Optics Communications 461 (2020) 125257

Contents lists available at ScienceDirect

Optics Communications

journal homepage: www.elsevier.com/locate/optcom

Gigahertz coherent longitudinal acoustic phonons in GaAs Single crystals with different orientations

Xiaobo Han [a], Mengya Wang [b], Wenchao Zhao [b], Xiangyuan Xing [b], Kai Wang [b,*], Peixiang Lu [a,b,c]

[a] Hubei Key Laboratory of Optical Information and Pattern Recognition, Wuhan Institute of Technology, Wuhan 430205, China
[b] Wuhan National Laboratory for Optoelectronics and School of Physics, Huazhong University of Science and Technology, Wuhan 430074, China
[c] CAS Center for Excellence in Ultra-intense Laser Science, Shanghai 201800, China

ARTICLE INFO

Keywords:
Coherent longitudinal acoustic phonons
GaAs single crystal
Ultrafast dynamics
Crystal orientation

ABSTRACT

We report an experimental study on the ultrafast dynamics of coherent longitudinal acoustic phonons (CLAPs) in GaAs single crystals with different orientations by using femtosecond pump–probe technique. Under an above-bandgap pumping at 400 nm, the CLAP wave is generated on the surface of a GaAs crystal with [100] orientation, and then it propagates into the crystal and is detected by the transient reflection of the probe beam at 800 nm. As the pumping intensity is increased, the amplitude and lifetime of generated CLAPs in GaAs crystals are increased and decreased respectively, while the phonons oscillation frequency remains a constant of 44.3±0.2 GHz. Furthermore, the CLAPs frequency is varied in GaAs crystals with different orientations which is determined by the elastic anisotropy. In addition, from the initially opposite oscillation phase of [100] and [111] oriented GaAs, tensile or compressive lattice stresses can be easily determined. Our results can facilitate the understanding of ultrafast phonon dynamics in GaAs single crystals.

1. Introduction

Advances in femtosecond lasers and ultrafast spectroscopy [1–6] allow us to generate and directly detect the coherent oscillation of phonon modes. In particular, coherent longitudinal acoustic phonons (CLAPs) excited by ultrashort optical pulses have been vastly investigated in semiconductors [7–10], metal films [11], multiple quantum wells [12] and heterostructures [8,13] by using pump–probe techniques. Femtosecond pump pulses are absorbed at sample surfaces, which initiates the generation of coherent phonons on the sample surface. Due to the interaction between the coherent phonons and the electronic or excitonic states, the refractive index and the reflectivity of the materials are modulated. Thus, the transient signals of coherent phonons can be detected by monitoring a reflected or transmitted time-delayed probe light. This technique not only avoids unwanted damage on the sample but also is sure to improve potential applications of nondestructive testing of CLAPs. Previous studies manifest four types of physical mechanisms of CLAPs generation: the deformation potential coupling stress [14,15], the heat-induced thermal stress [10,16], the inverse piezoelectric effect [17,18], and the electrostriction [19,20].

GaAs is one of the most studied semiconducting materials [21–27] with excellent traits, such as a stable zinc blende structure, high resistivity and ultrahigh electron mobility. These excellent traits make GaAs to apply in all sorts of photonic devices. Furthermore, GaAs is a direct band gap semiconductor with the band gap of 1.43 eV at room temperature [28], which makes the materials a choice for high-efficiency solar cells [29]. Therefore, it is worth investigating the ultrafast dynamics in GaAs single crystals. Coherent phonons have been investigated in multiple quantum wells, superlattices and alloys based on GaAs (e.g., InGaAs/GaAs, GaSb/GaAs, GaAs/AlAs) [8,30–32]. However, a common feature of such structures is the highly strained interfaces due to an apparent lattice mismatch, making the dominant contribution on the phonon generation. Therefore, it should be ignored for the phonons generation in high quality GaAs single crystals, which are mainly ascribed to the deformation potential coupling and thermal stresses.

In this paper, we investigate the ultrafast dynamics of CLAPs in GaAs single crystals with different orientations of [100], [110], [111] and Si-doped [100] by using pump–probe technique. The CLAPs oscillation wave is generated on the surface of GaAs single crystal under an above-bandgap pumping at 400 nm. And then, it propagates into the crystal and is detected by a time-delayed probe light at 800 nm. With increasing the pump intensities, the amplitude and lifetime of acoustic phonons in GaAs single crystals are increased and decreased, respectively. A fast oscillation at gigahertz frequency (44.3 ± 0.2 GHz) of CLAPs is observed in [100] oriented GaAs crystals at room temperature. And the oscillation frequency is independent on the pumping intensity. In addition, the CLAPs frequencies are varied in GaAs single crystals with different orientations, which are attributed to the elastic

* Corresponding author.
E-mail address: kale_wong@hust.edu.cn (K. Wang).

https://doi.org/10.1016/j.optcom.2020.125257
Received 31 July 2019; Received in revised form 26 December 2019; Accepted 4 January 2020
Available online 7 January 2020

anisotropy of GaAs crystal. Furthermore, from the initially opposite oscillation phase of [100] and [111] oriented GaAs, tensile or compressive lattice stresses can be easily determined. It offers new experimental evidence for understanding the ultrafast phonon dynamics in GaAs single crystals.

2. Material and method

The 0.5-mm thick GaAs single crystals with different orientations of [100], [110], [111] and Si-doped [100] (Si-doped to 1.8×10^{18} cm^{-3}) were purchased from KJMT. All samples have single-sided polished surfaces with zinc blende structure. A regeneratively amplified Ti: sapphire laser (Astrella, Coherent, 35 fs, 1 kHz) with a center wavelength of 800 nm was primary excitation source for pump–probe measurement. A portion of the beam was split off to serve as the probe beam and the remaining beam was frequency doubled by a BBO crystal to produce a pump beam at 400 nm. The pump beam was incident obliquely at an angle of ~60° and was focused through a 10-cm lens. The lengths of long and short axes of the elliptic spot were about 200 μm and 50 μm, respectively. The probe beam at 800 nm is delayed in time with respect to the pump beam and normally focused onto the same position with the pump beam by an objective (Thorlabs, 4×/0.13 PhL). The diameter of probe beam spot was ~20 μm, which is smaller than the pump beam spot. In order to improve the signal to noise ratio (SNR), a balanced photodiode detector (Thorlabs, PDB210A/M) connected to a lock-in amplifier (Stanford, SR830) was used to collect the reflected probe beam. The pump beam was modulated at ~470 Hz by a mechanical chopper. All the experiments are measured at room temperature.

3. Results and discussion

Fig. 1(a) displays the transient reflectivity signals obtained in [100] oriented GaAs crystal at different pump fluences. The three traces present similar results consisting of decays and oscillations. In the first several picoseconds, an abrupt rise of $\Delta R/R$ is observed which can be attributed to the change of refractive index induced by the pump photon-excited electron–hole pairs. As can be seen from the inset, there is an enhancement of signal intensity as increasing the pump fluences. Then the photo-excited carriers transfer their excess energy to the lattices, leading to the long-time decays. To obtain the decay times of the electrons and phonons, we fit the observed traces with a set of decaying exponential functions:

$$\Delta R/R \propto R_e + R_{CLAP} = \sum_{i=1}^{2} A_{ei} e^{-t/\tau_{ei}} + A_{ph} e^{-t/\tau_{ph}} \cos[(\omega + \beta t)t + \varphi] \quad (1)$$

where A_{ei} and τ_{ei} are the amplitude and decay time of electron relaxation processes in the ith component, respectively. A_{ph} is the amplitude of coherent oscillations, τ_{ph} is the lifetime of phonons, ω denotes the CLAP oscillation frequency, β is the chirping coefficient and φ is the initial phase. The electrons response can be fitted by a biexponential function of the electron term R_e of Eq. (1). Two exponential curves indicate the fast and slow electronic relaxations, respectively [9,33].

Fig. 1(b) presents the peak intensity of $\Delta R/R$ as a function of the pump fluences. It indicates that the maximum value of $\Delta R/R$ increases gradually as the growth of pump fluences, and then the value tends to be relatively stable. This trend is probably attributed to the fact that the carrier concentration first increases rapidly with increasing the pump fluences, and then it reaches a steady state due to the competition between carrier generation and recombination. The peak intensity $(\Delta R/R)_{max}$ is usually related to the maximum carriers temperature, since the photo-excited carriers transfer their excess energy to the lattices. Fig. 1(c) shows the fast electronic decay time at different pump fluences, and it increases with high pump fluence. The timescale of τ_{e1} is consistent with the trapping time of free electrons in bulk GaAs according to previous studies [34–36]. Thus, it may be explained by rapid trapping of electrons from the conduction band into mid-gap states. Since the occupancy of defect states begins to saturate with higher pump fluence, τ_{e1} increases as pump fluence increasing [37,38]. However, the trend of the slow electronic decay time decreases almost linearly as increasing the pump fluences in Fig. 1(d). It can be attributed to that high pump fluence leads to strong absorption and higher concentrations of carriers, which increases the probability of recombination [39–41]. The electronic decay time is very sensitive to temperature which is interrelated with the pump fluences.

In Fig. 1(a), the whole decay contains both electrons and coherent phonons responses. In order to obtain the pure oscillations of CLAPs, the electronic background is subtracted from raw data. The extracted CLAP signals and their fitting results are presented in Fig. 2(a). The oscillations of CLAPs are fitted using an exponentially damped oscillation function, namely the phonon term R_{CLAP} of Eq. (1). Furthermore, the oscillations in Fig. 2(a) are attenuated, whereas their periods maintain all the same among 350 ps delay time. The origin of the transient reflectivity of oscillations is explained first by Thomsen *el at* [42]. In picosecond ultrasonic, propagating CLAPs are detected through Brillouin oscillations. The CLAP oscillations come from the interference of probe beam between the reflection at the sample surface and its reflection at the CLAP strained layer. In order to obtain the oscillation frequency of CLAPs exactly, the fast Fourier transform (FFT) of the transient reflectivity after removing the electronic background is done. As shown in Fig. 2(b), it shows only one peak frequency of the Brillouin oscillations at each pump fluences. Moreover, comparing with the frequency of optical phonons [43], it can be observed that there is a same single frequency (44.3 ± 0.2 GHz) for [100] oriented GaAs crystals at different pump fluences. It confirms that the oscillation frequency of CLAPs is only related to the refractive index of material and the wavelength of probe light, which can be expressed as [42]:

$$f = n v_s K_{probe} / \pi = 2 n v_s / \lambda_{prove} \quad (2)$$

where n is the refractive index, which is 3.67 at 800 nm probe wavelength in GaAs [44], v_s is the longitudinal acoustic phonons velocity, and k_{probe} is the wave vector of probe beam.

We observe a variation of the amplitude of the generated CLAPs at different pump fluences, plotted in Fig. 3(a). The amplitude of CLAPs increases near-linearly at low fluences, while it saturates at high fluences. According to Hooke's law [45], the amplitude of CLAPs generated by the light absorption is proportional to the stress within the sample. The optical absorption depth of GaAs (ξ = 15 nm at 3.1 eV) is small enough compared to the laser spot size to allow a one-dimensional treatment of the acoustic perturbation. For the nonpiezoelectrically active [100] oriented GaAs single crystals, the transient stress includes deformation potential coupling stress (electronic stress) and thermal stress. Thus, the contributions of generated stress due to the absorption of single laser pulses can be expressed as [46]:

$$\sigma = \sigma_{DP} + \sigma_{TE} = -NB\left(\frac{dE_g}{dP} + 3\kappa\frac{h\nu - E_g}{C_p}\right) \quad (3)$$

where σ_{DP} and σ_{TE} indicate the contributions of the deformation potential and thermoelasticity to stress, respectively. N is the density of photo-excited carriers, B is the bulk modulus, dE_g/dP is the hydrostatic deformation potential parameter, κ is the linear thermal expansion coefficient, $h\nu$ is the energy of pump photon energy, E_g is the bandgap of GaAs and C_P is the heat capacity. The ratio between the electronic and thermal strains is approximately $(dE_g/dP)C_p/[3\kappa(h\nu - E_g)] \approx 5.8$, indicating that the dominant stress is σ_{DP}. Note that after the laser pulse absorption, the speed, v_n, of optically excited carriers in GaAs initially exceeds the longitudinal sound velocity, c_a. It results in that the strain pulse duration caused by σ_{DP} will longer than that only localized in the region of optical absorption length (Δt = 6 ps) [14,47]. According to Eq. (3), at low fluences, the amplitude magnitude of CLAPs, A_{ph}, increases linearly which is closely associated to the initially pump excited carrier density, N. The slow increasing rate at high fluences

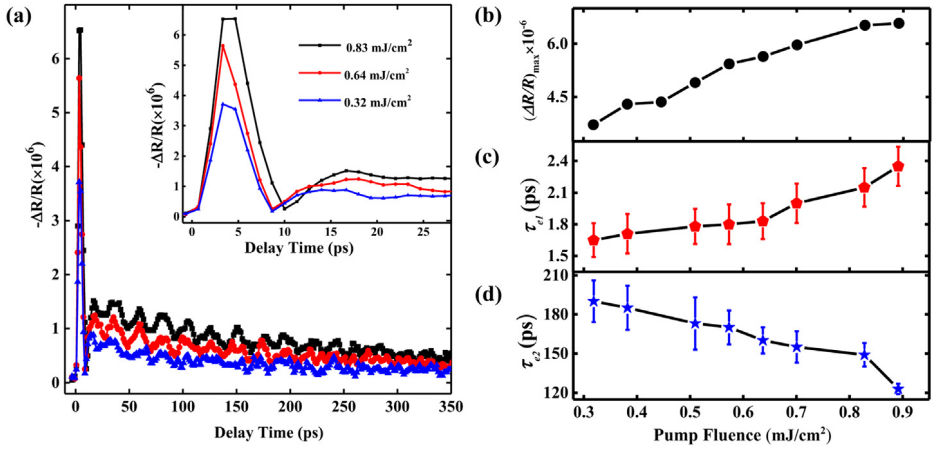

Fig. 1. (a) Transient reflectivity signals for [100] oriented GaAs crystal at different pump fluences at a picosecond time scale. Inset shows an expanded view (between −2~28 ps) of the transient reflectivity signals. (b) The maximum values of $\Delta R/R$ as a function of pump fluences. (c, d) The fast electronic decay time τ_{e1} and the slow electronic decay time τ_{e2} at different pump fluences, respectively.

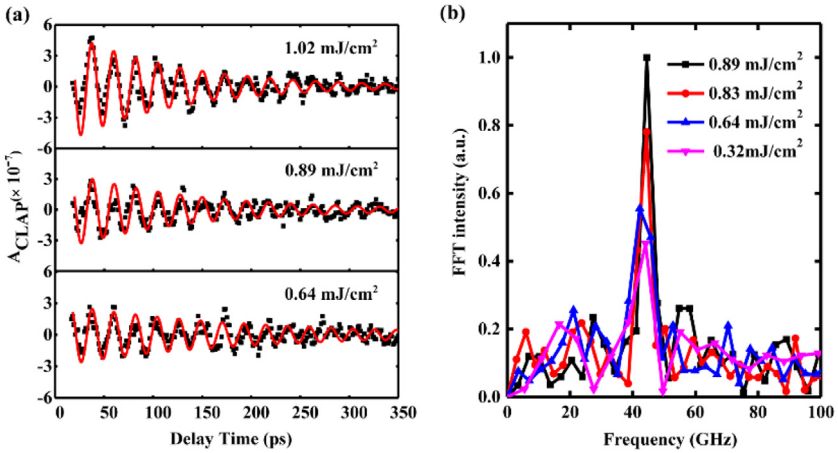

Fig. 2. (a) Extracted CLAP oscillations (black squares) for [100] oriented GaAs single crystal and their fitting results (red line) at the pump fluences of 1.02 mJ/cm^2, 0.89 mJ/cm^2, and 0.64 mJ/cm^2, respectively. A_{CLAP} is the amplitude of the coherent phonons. (b) The fast Fourier transform (FFT) of CLAP oscillations for [100] oriented GaAs crystal at different fluences.

may be a result of two competing effects: deviation from the linearity of the pump-induced absorption at high pump fluences, and a rapid rise of lattice temperature at high fluences. Fig. 3(b) shows a slow decrease of CLAPs lifetime as increasing the pump fluences, which is the result of the increased carrier scattering. It is worth noting that it is important to include the variation of the phonon frequency with time (chirped coefficient β) in the oscillations fitting. Without considering β, the fitting results are inconsistent with the experimental data. The value of β is shown in Fig. 3(c), and its order of magnitude is about 10^{-6}. Comparing with coherent optical phonons, their chirped coefficient β ($\sim 10^{-1}$) [43] is five orders of magnitude larger than β ($\sim 10^{-6}$) of acoustic phonons. Small values of β indicate that the deformation of CLAPs is negligible.

In order to investigate the effect of crystal orientation on phonon oscillation process, another two orientated GaAs crystals of [110] and [111] are investigated. The fluence dependences are almost same for [110] and [111] oriented crystals as observed in Fig. 1(b–d) and Fig. 3 for the [100] oriented crystal. Fig. 4 presents the extracted oscillations and normalized FFT results for these three oriented GaAs crystals. Considering that the measured pump fluence is much higher than the piezoelectric contribution saturated threshold value (at fluence of 18–45 μJ/cm^2) [18,48], the CLAP generation mechanism can be seen as the same for three oriented crystals. In Fig. 4(b), the oscillation frequency is varied for different orientated crystals, and then we try to calculate the frequency in theory. Due to the zinc blende GaAs belongs to cubic

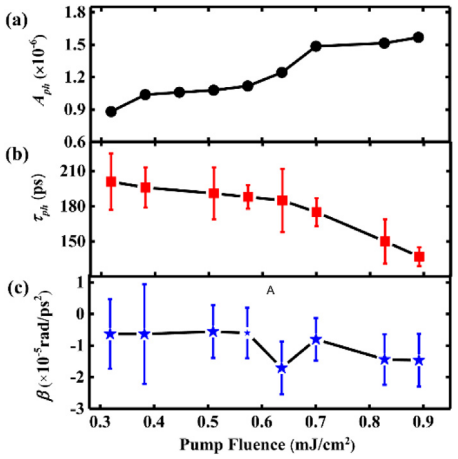

Fig. 3. CLAP properties for [100] oriented GaAs crystal at different pump fluences: (a) amplitude A_{ph}, (b) decay time τ_{ph} and (c) chirp coefficient β.

crystals, there are three independent elasticity tensor components C_{11} = 124.2 GPa, C_{12} = 51.4 GPa, and C_{44} = 63.4 GPa [49]. These components are used to determine the complete elastic tensor of the material.

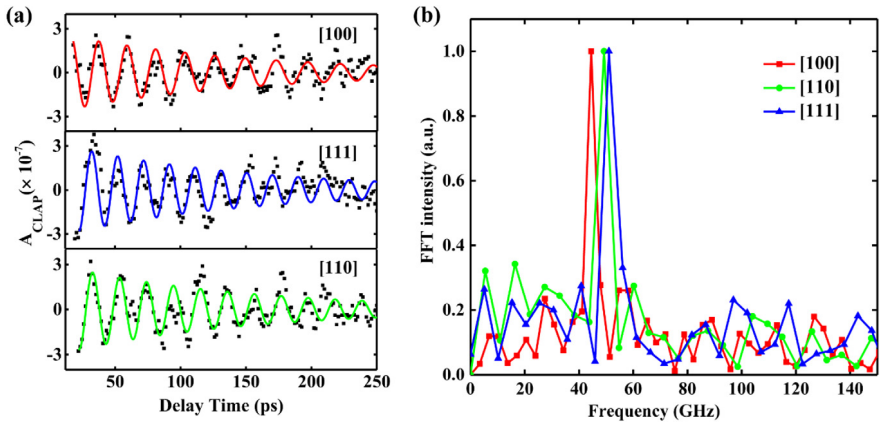

Fig. 4. (a) Extracted CLAP oscillations (black squares) for [100], [111] and [110] oriented GaAs single crystals and their fitting results (lines) at pump fluences of 0.64 mJ/cm^2, 0.75 mJ/ cm^2, and 0.69 mJ/ cm^2, respectively. A_{CLAP} is the amplitude of the coherent phonons. (b) FFT of CLAP oscillations corresponding to (a).

Table 1
The theoretical and experimental oscillation frequencies of zinc blende GaAs with different orientations.

Crystal orientation	[100]	[110]	[111]
Theory (GHz)	44.2	48.7	50.2
Experiment (GHz)	44.3 ± 0.2	49.3 ± 0.22	51.0 ± 0.25

For the zinc blende structure, the relations between the longitudinal sound velocity and elasticity can be expressed as: $\upsilon_s = \sqrt{C/\rho}$, where $\rho = 5360$ kg cm^{-3} is the mass density for GaAs crystals [50], and C is the effective elastic constant. For the [100], [110] and [111] oriented GaAs crystals, the effective elastic constants of the longitudinal wave are C_{11}, $1/2(C_{11} + C_{12}+2C_{44})$ and $1/3(C_{11}+2C_{12}+4C_{44})$, respectively. Thus, we can use Eq. (2) to calculate the CLAP oscillations frequency. As shown in Table 1, the theoretical results are in good agreement with the experimental ones. Therefore, combined with experimental and theoretical results, we proved that the CLAPs oscillation frequency is determined by elastic properties.

It is worth noting that in first several oscillation cycles of Fig. 4(a), the phonon phase of the [100] and [111] oriented GaAs is opposite. It indicated that the initiated stress is tensile and compressive for [100] and [111] orientations, respectively [46]. Depending on the nature of the electronic levels where the electrons (and holes) are photo-promoted, the lattice stress can be compressive or tensile. When electrons are promoted in the Γ ($dE_g/dP = 10$ eV/Mbar) and L valley ($d(E_L - E_\Gamma)/dP = 5.5$ eV/Mbar) of GaAs, it helps to expand the crystal. On the contrary, it contributes to a shrinkage when electrons are promoted in the X valley ($d(E_X - E_\Gamma)/dP = -2.5$ eV/Mbar). We remind that E_Γ is the highest energy in the valence band, E_L and E_X are the energy minima of the conduction bands situated respectively along the directions [111] and [100] in the Brillouin zone. Hence, it demonstrates that the opposite deformational potential coupling stress is dominated in [111] and [100] direction GaAs and leads the observed initially opposite phase. The similarly initial phase of [111] and [110] orientations are shown, which may implicate the same sign of lattice stresses.

In addition, we measure the CLAPs from Si-doped [100] oriented GaAs, and the phonons oscillation frequency is around 43.7 ± 0.15 GHz. Comparing with the un-doped GaAs, the Brillouin frequency is slightly decreased. Since the elastic tensors determine the oscillation frequency, we assume that the varied frequency in dopant GaAs is essentially due to the changed elastic property. For the doped materials, dopant atoms substituting original atoms modify the electron distributions. And the elastic property is basically determined by the interactions of electrons [51]. Therefore, doping further leads to change the elastic tensors [52,53]. The change of refractive index is usually very small that can be ignored. Thus, the decreased phonon oscillation frequency of Si-doped GaAs crystals can be attributed to the varied elastic property. More experimental and theoretical researches need to be done for further investigating the relationship between doping and phonon frequency shift.

4. Conclusion

In summary, we investigate the ultrafast dynamics of CLAPs in GaAs single crystals with different orientations of [100], [110], [111] and Si-doped [100] by using two-color femtosecond pump–probe technique. Under the above-bandgap pumping light at 400 nm, the CLAPs are generated on the surface of GaAs crystals and subsequently propagates into the crystals. A time-delayed probe beam at 800 nm monitors the relative variation of reflectivity. The picosecond coherent phonons oscillations in GaAs crystal at different pump fluences are detected, which comes from the deformation potential coupling and thermal stresses. With increasing the pump fluences, the amplitude and lifetime of CLAPs are increased and decreased respectively, while the phonon oscillation frequency remains a constant of 44.3 ± 0.2 GHz. Additionally, in experiment and theory we show the oscillation frequency is varied with different orientations of GaAs crystals. And it is confirmed that the elastic anisotropy of GaAs crystals determines the changed oscillation frequency. Furthermore, from the initially opposite oscillation phase of [100] and [111] GaAs, tensile or compressive lattice stresses can be easily determined. The results can facilitate the understanding of ultrafast phonon dynamics in GaAs single crystals. The femtosecond pump–probe technique makes it possible to successfully generate nanoscale acoustic waves at the sample surface and be utilized as a nondestructive tool to measure deep layers.

CRediT authorship contribution statement

Xiaobo Han: Methodology, Data curation, Writing - original draft, Writing - review & editing. **Mengya Wang:** Visualization, Validation, Investigation, Formal analysis, Writing - original draft. **Wenchao Zhao:** Resources, Validation. **Xiangyuan Xing:** Resources, Data curation. **Kai Wang:** Conceptualization, Investigation, Writing - review & editing, Supervision. **Peixiang Lu:** Conceptualization, Writing - review & editing, Project administration, Supervision.

Acknowledgments

This work was supported by National Natural Science Foundation of China (nos., 11774115 and 91850113) and the 973 Programs, China under grants 2014CB921301 and the Campus Science Foundation Research Project of Wuhan Institute of Technology, China (No. K201822).

Special thanks to the Analytical and Testing Center of HUST and the Center of Micro-Fabrication and Characterization (CMFC) of WNLO for using their facilities. Thanks to the facility support of the Center for Nanoscale Characterization & Devices (CNCD), WNLO of HUST.

References

[1] R.W. Schoenlein, S. Chattopadhyay, H.H. Chong, T.E. Glover, P.A. Heimann, C.V. Shank, A.A. Zholents, M.S. Zolotorev, Generation of femtosecond pulses of synchrotron radiation, Science 287 (2000) 2237–2240.

[2] Z. Hong, S.A. Rezvani, Q. Zhang, P. Lu, Ultrafast Mid-IR laser pulses generation via chirp manipulated optical parametric amplification, Appl. Sci.-Basel 8 (2018) 744.

[3] H. Yuan, L. He, F. Wang, B. Wang, W. Liu, Z. Hong, Generation of isolated attosecond pulses in a multi-cycle inhomogeneous two-color field without CEP stabilization, Opt. Quantum Electron. 49 (2017) 214.

[4] Z. Hong, Q. Zhang, S.A. Rezvani, P. Lan, P. Lu, Tunable few-cycle pulses from a dual-chirped optical parametric amplifier pumped by broadband laser, Opt. Laser Technol. 98 (2018) 169–177.

[5] B. Wang, L. He, Y. He, Y. Zhang, R. Shao, P. Lan, P. Lu, All-optical measurement of high-order fractional molecular echoes by high-order harmonic generation, Opt. Express 27 (2019) 30172–30181.

[6] Z. Yang, W. Cao, X. Chen, J. Zhang, Y. Mo, H. Xu, K. Mi, Q. Zhang, P. Lan, P. Lu, All-optical frequency resolved optical gating for isolated attosecond pulse reconstruction, arXiv preprint arXiv:1911.06427.

[7] D.H. Feng, X.Q. Pan, X. Li, T.Q. Jia, Z.R. Sun, Coherent acoustic phonon generation and detection by femtosecond laser pulses in ZnTe single crystals, J. Appl. Phys. 114 (2013) 093513.

[8] K.L. Pollock, H.Q. Doan, A. Rustagi, C.J. Stanton, T. Cuk, Detecting the photoexcited carrier distribution across GaAs/transition metal oxide interfaces by coherent longitudinal acoustic phonons, J. Phys. Chem. Lett. 8 (2017) 922–928.

[9] W. Wu, Y. Wang, Ultrafast carrier dynamics and coherent acoustic phonons in bulk CdSe, Opt. Lett. 40 (2015) 64–67.

[10] S. Wu, P. Geiser, J. Jun, J. Karpinski, R. Sobolewski, Femtosecond optical generation and detection of coherent acoustic phonons in GaN single crystals, Phys. Rev. B 76 (2007) 085210.

[11] C. Rossignol, J.M. Rampnoux, M. Perton, B. Audoin, S. Dilhaire, Generation and detection of shear acoustic waves in metal submicrometric films with ultrashort laser pulses, Phys. Rev. Lett. 94 (2005) 166106.

[12] C.K. Sun, J.C. Liang, X.Y. Yu, Coherent acoustic phonon oscillations in semiconductor multiple quantum wells with piezoelectric fields, Phys. Rev. Lett. 84 (2000) 179–182.

[13] C. He, M. Daniel, M. Grossmann, O. Ristow, D. Brick, M. Schubert, M. Albrecht, T. Dekorsy, Dynamics of coherent acoustic phonons in thin films of $CoSb_3$ and partially filled $Yb_xCo_4Sb_{12}$ skutterudites, Phys. Rev. B 89 (2014) 174303.

[14] O.B. Wright, B. Perrin, O. Matsuda, V.E. Gusev, Ultrafast carrier diffusion in gallium arsenide probed with picosecond acoustic pulses, Phys. Rev. B 64 (2001) 081202.

[15] K. Ishioka, A. Rustagi, U. Höfer, H. Petek, C.J. Stanton, Intrinsic coherent acoustic phonons in the indirect band gap semiconductors Si and GaP, Phys. Rev. B 95 (2017) 035205.

[16] P.A. Mante, C.C. Stoumpos, M.G. Kanatzidis, A. Yartsev, Electron-acoustic phonon coupling in single crystal $CH_3NH_3PbI_3$ perovskites revealed by coherent acoustic phonons, Nature Commun. 8 (2017) 14398.

[17] K.-H. Lin, C.-T. Yu, Y.-C. Wen, C.-K. Sun, Generation of picosecond acoustic pulses using a p–n junction with piezoelectric effects, Appl. Phys. Lett. 86 (2005) 093110.

[18] G. Vaudel, T. Pezeril, A. Lomonosov, M. Lejman, P. Ruello, V. Gusev, Laser generation of hypersound by a terahertz photo-Dember electric field in a piezoelectric GaAs semiconductor, Phys. Rev. B 90 (2014) 014302.

[19] V. Gusev, P. Picart, D. Mounier, J.M. Breteau, On the possibility of ultrashort shear acoustic pulse excitation due to the laser-induced electrostrictive effect, Opt. Commun. 204 (2002) 229–236.

[20] Y.X. Yan, E.B. Gamble, K.A. Nelson, Impulsive stimulated scattering: General importance in femtosecond laser pulse interactions with matter, and spectroscopic applications, J. Chem. Phys. 83 (1985) 5391–5399.

[21] X. Han, K. Wang, H. Long, H. Hu, J. Chen, B. Wang, P. Lu, Highly sensitive detection of the lattice distortion in single bent ZnO nanowires by second-harmonic generation microscopy, ACS Photonics 3 (2016) 1308–1314.

[22] H. Long, L. Bao, A.A. Habeeb, P. Lu, Effects of doping concentration on the surface plasmonic resonances and optical nonlinearities in AGZO nano-triangle arrays, Opt. Quantum Electron. 49 (2017) 345.

[23] M. Timofeeva, A. Bouravleuv, G. Cirlin, I. Shtrom, I. Soshnikov, M. Reig Escalé, A. Sergeyev, R. Grange, Polar second-harmonic imaging to resolve pure and mixed crystal phases along GaAs nanowires, Nano Lett. 16 (2016) 6290–6297.

[24] W. Liu, X. Li, Y. Song, C. Zhang, X. Han, H. Long, B. Wang, K. Wang, P. Lu, Cooperative enhancement of two-photon-absorption-induced photoluminescence from a 2D perovskite-microsphere hybrid dielectric structure, Adv. Funct. Mater. 28 (2018) 1707550.

[25] J. Chen, K. Wang, K. Wu, L. Qian, H. Long, B. Wang, P. Lu, Optimization of metal-enhanced fluorescence by different concentrations of gold-silica core–shell nanoparticles, Opt. Commun. 349 (2015) 180–184.

[26] J. Chen, K. Wang, H. Long, X. Han, H. Hu, W. Liu, B. Wang, P. Lu, Tungsten disulfide-gold nanohole hybrid metasurfaces for nonlinear metalenses in the visible region, Nano Lett. 18 (2018) 1344–1350.

[27] X. Li, W. Liu, Y. Song, H. Long, K. Wang, B. Wang, P. Lu, Two-photon-pumped high-quality, single-mode vertical cavity lasing based on perovskite monocrystalline films, Nano Energy 68 (2020) 104334.

[28] H. Ohno, A. Shen, F. Matsukura, A. Oiwa, A. Endo, S. Katsumoto, Y. Iye, (Ga, Mn)As: A new diluted magnetic semiconductor based on GaAs, Appl. Phys. Lett. 69 (1996) 363–365.

[29] I. Aberg, G. Vescovi, D. Asoli, U. Naseem, J.P. Gilboy, C. Sundvall, A. Dahlgren, K.E. Svensson, N. Anttu, M.T. Bjork, L. Samuelson, A GaAs nanowire array solar cell with 15.3% efficiency at 1 sun, IEEE J. Photovolt. 6 (2016) 185–190.

[30] Y.-C. Wen, L.-C. Chou, H.-H. Lin, V. Gusev, K.-H. Lin, C.-K. Sun, Efficient generation of coherent acoustic phonons in (111) InGaAs/GaAs multiple quantum wells through piezoelectric effects, Appl. Phys. Lett. 90 (2007) 172102.

[31] Y. Xu, J. Qi, J. Miller, Y.J. Cho, X. Liu, J.K. Furdyna, T.V. Shahbazyan, N. Tolk, Pump-probe studies of travelling coherent longitudinal acoustic phonon oscillations in GaAs, Phys. Status Solidi (c) 5 (2008) 2632–2636.

[32] A. Huynh, B. Perrin, A. Lemaitre, Semiconductor superlattices: a tool for terahertz acoustics, Ultrasonics 56 (2015) 66–79.

[33] D. Hsieh, F. Mahmood, D.H. Torchinsky, G. Cao, N. Gedik, Observation of a metal-to-insulator transition with both Mott-Hubbard and Slater characteristics in Sr_2IrO_4 from time-resolved photocarrier dynamics, Phys. Rev. B 86 (2012) 035128.

[34] P. Grenier, J.F. Whitaker, Subband gap carrier dynamics in low-temperature-grown GaAs, Appl. Phys. Lett. 70 (1997) 1998–2000.

[35] T.S. Sosnowski, T.B. Norris, H.H. Wang, P. Grenier, J.F. Whitaker, C.Y. Sung, High-carrier-density electron dynamics in low-temperature-grown GaAs, Appl. Phys. Lett. 70 (1997) 3245–3247.

[36] I.S. Gregory, C.M. Tey, A.G. Cullis, M.J. Evans, H.E. Beere, I. Farrer, Two-trap model for carrier lifetime and resistivity behavior in partially annealed GaAs grown at low temperature, Phys. Rev. B 73 (2006) 195201.

[37] H. Liu, J. Lu, H.F. Teoh, D. Li, Y.P. Feng, S.H. Tang, C.H. Sow, X. Zhang, Defect engineering in CdS_xSe_{1-x} nanobelts: An insight into carrier relaxation dynamics via optical pump–Terahertz probe spectroscopy, J. Phys. Chem. C 116 (2012) 26036–26042.

[38] P. Parkinson, H.J. Joyce, Q. Gao, H.H. Tan, X. Zhang, J. Zou, C. Jagadish, L.M. Herz, M.B. Johnston, Carrier lifetime and mobility enhancement in nearly defect-free core-shell nanowires measured using time-resolved Terahertz spectroscopy, Nano Lett. 9 (2009) 3349–3353.

[39] S.S. Li, Semiconductor Physical Electronics, Springer Science & Business Media, 2006.

[40] W. Wu, Z. Chai, Y. Gao, D. Kong, F. He, X. Meng, Y. Wang, Carrier dynamics and optical nonlinearity of alloyed CdSeTe quantum dots in glass matrix, Opt. Mater. Express 7 (2017) 1547.

[41] C. Wehrenfennig, G.E. Eperon, M.B. Johnston, H.J. Snaith, L.M. Herz, High charge carrier mobilities and lifetimes in organolead trihalide perovskites, Adv. Mater. 26 (2014) 1584–1589.

[42] C. Thomsen, H.T. Grahn, H.J. Maris, J. Tauc, Surface generation and detection of phonons by picosecond light pulses, Phys. Rev. B 34 (1986) 4129–4138.

[43] A.Q. Wu, X. Xu, Coherent phonon excitation in bismuth, Appl. Surf. Sci. 253 (2007) 6301–6304.

[44] D.E. Aspnes, S.M. Kelso, R.A. Logan, R. Bhat, Optical properties of $Al_xGa_{1-x}As$, J. Appl. Phys. 60 (1986) 754–767.

[45] D. Royer, E. Dieulesaint, Advanced texts in physics springer, 2000.

[46] P. Ruello, V.E. Gusev, Physical mechanisms of coherent acoustic phonons generation by ultrafast laser action, Ultrasonics 56 (2015) 21–35.

[47] E.S.K. Young, A.V. Akimov, R.P. Campion, A.J. Kent, V. Gusev, Picosecond strain pulses generated by a supersonically expanding electron–hole plasma in GaAs, Phys. Rev. B 86 (2012) 155207.

[48] P. Babilotte, P. Ruello, T. Pezeril, G. Vaudel, D. Mounier, J.M. Breteau, V. Gusev, Transition from piezoelectric to deformation potential mechanism of hypersound photogeneration in n-doped GaAs semiconductors, J. Appl. Phys. 109 (2011) 064909.

[49] S.Q. Wang, H.Q. Ye, First-principles study on elastic properties and phase stability of III-V compounds, Phys. Status Solidi b 240 (2003) 45–54.

[50] O. Matsuda, T. Tachizaki, T. Fukui, J.J. Baumberg, O.B. Wright, Acoustic phonon generation and detection in $GaAs/Al_{0.3}Ga_{0.7}As$ quantum wells with picosecond laser pulses, Phys. Rev. B 71 (2005) 115330.

[51] R.W. Keyes, Elastic properties of diamond-type semiconductors, J. Appl. Phys. 33 (1962) 3371–3372.

[52] Z. Rak, S.D. Mahanti, K.C. Mandal, N.C. Fernelius, Doping dependence of electronic and mechanical properties of $GaSe_{1-x}Te_x$ and $Ga_{1-x}In_xSe$ from first principles, Phys. Rev. B 82 (2010) 155203.

[53] A. Kumar, A. Chernatynskiy, M. Hong, S.R. Phillpot, S.B. Sinnott, An ab initio investigation of the effect of alloying elements on the elastic properties and magnetic behavior of Ni_3Al, Comput. Mater. Sci. 101 (2015) 39–46.